Inorganic Chemistry

Article

pubs.acs.org/IC

Development of a Gd(III)-Based Receptor-Induced Magnetization Enhancement (RIME) Contrast Agent for β-Glucuronidase Activity Profiling

Shih-Hsien Chen,[†,‡,○] Yu-Ting Kuo,[‡,§,○] Gyan Singh,[#] Tian-Lu Cheng,[∥] Yu-Zheng Su,[⊥] Tzu-Pin Wang,[⊥] Yen-Yu Chiu,[‡] Jui-Jen Lai,[‡] Chih-Ching Chang,[‡] Twei-Shiun Jaw,[‡,§] Shey-Cherng Tzou,[#] Gin-Chung Liu,[*,‡,§] and Yun-Ming Wang[*,#]

[†]Graduate Institute of Medicine, College of Medicine, Kaohsiung Medical University, 100 Shih-Chuan first Road, Kaohsiung 807, Taiwan

[‡]Department of Medical Imaging, Kaohsiung Medical University Hospital, Kaohsiung, Taiwan

[§]Department of Radiology, Faculty of Medicine, College of Medicine, Kaohsiung Medical University, 100 Shih-Chuan first Road, Kaohsiung 807, Taiwan

[∥]Department of Biomedical Science and Environmental Biology, College of Life Sciences, Kaohsiung Medical University, 100 Shih-Chuan first Road, Kaohsiung 807, Taiwan

[⊥]Department of Medicinal and Applied Chemistry, Kaohsiung Medical University, Kaohsiung 807, Taiwan

[#]Department of Biological Science and Technology, Institute of Molecular Medicine and Bioengineering, National Chiao Tung University, 75 Bo-Ai Street, Hsinchu, 300, Taiwan

Supporting Information

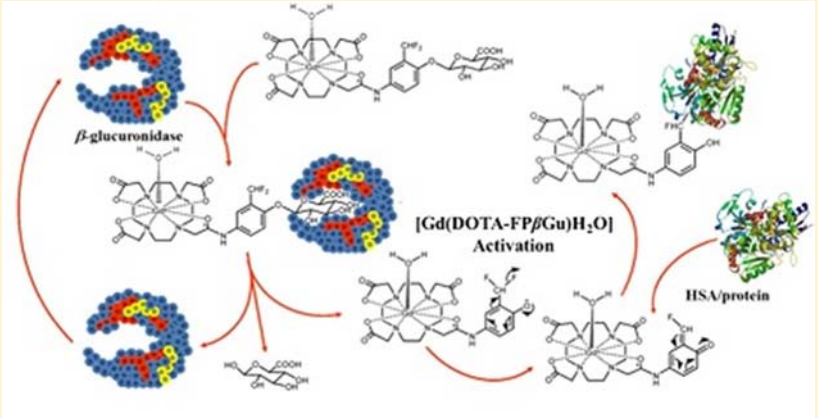

Systematic representation of β-glucuronidase induced transformation of pro-RIME [Gd(DOTA-FPβGu)] into ([Gd(DOTA-FP)]-HSA).

ABSTRACT: β-Glucuronidase is a key lysosomal enzyme and is often overexpressed in necrotic tumor masses. We report here the synthesis of a pro receptor-induced magnetization enhancement (pro-RIME) magnetic resonance imaging (MRI) contrast agent ([Gd(DOTA-FPβGu)]) for molecular imaging of β-glucuronidase activity in tumor tissues. The contrast agent consists of two parts, a gadolinium complex and a β-glucuronidase substrate (β-D-glucopyranuronic acid). The binding association constant (K_A) of [Gd(DOTA-FPβGu)] is 7.42×10^2, which is significantly lower than that of a commercially available MS-325 (K_A = 3.0×10^4) RIME contrast agent. The low K_A value of [Gd(DOTA-FPβGu)] is due to the pendant β-D-glucopyranuronic acid moiety. Therefore, [Gd(DOTA-FPβGu)] can be used for detection of β-glucuronidase through RIME modulation. The detail mechanism of enzymatic activation of [Gd(DOTA-FPβGu)] was elucidated by LC-MS. The kinetics of β-glucuronidase catalyzed hydrolysis of [Eu(DOTA-FPβGu)] at pH 7.4 best fit the Miechalis−Menten kinetic mode with K_m = 1.38 mM, k_{cat} = 3.76×10^3, and $k_{cat}/K_m = 2.72 \times 10^3$ M^{-1} s^{-1}. The low K_m value indicates high affinity of β-glucuronidase for [Gd(DOTA-FPβGu)] at physiological pH. Relaxometric studies revealed that T_1 relaxivity of [Gd(DOTA-FPβGu)] changes in response to the concentration of β-glucuronidase. Consistent with the relaxometric studies, [Gd(DOTA-FPβGu)] showed significant change in MR image signal in the presence of β-glucuronidase and HSA. *In vitro* and *in vivo* MR images demonstrated appreciable differences in signal enhancement in the cell lines and tumor xenografts in accordance to their expression levels of β-glucuronidase.

Received: August 21, 2012
Published: November 1, 2012

Scheme 1. Schematic Representation of the Synthesis of DOTA-FPβGu[a]

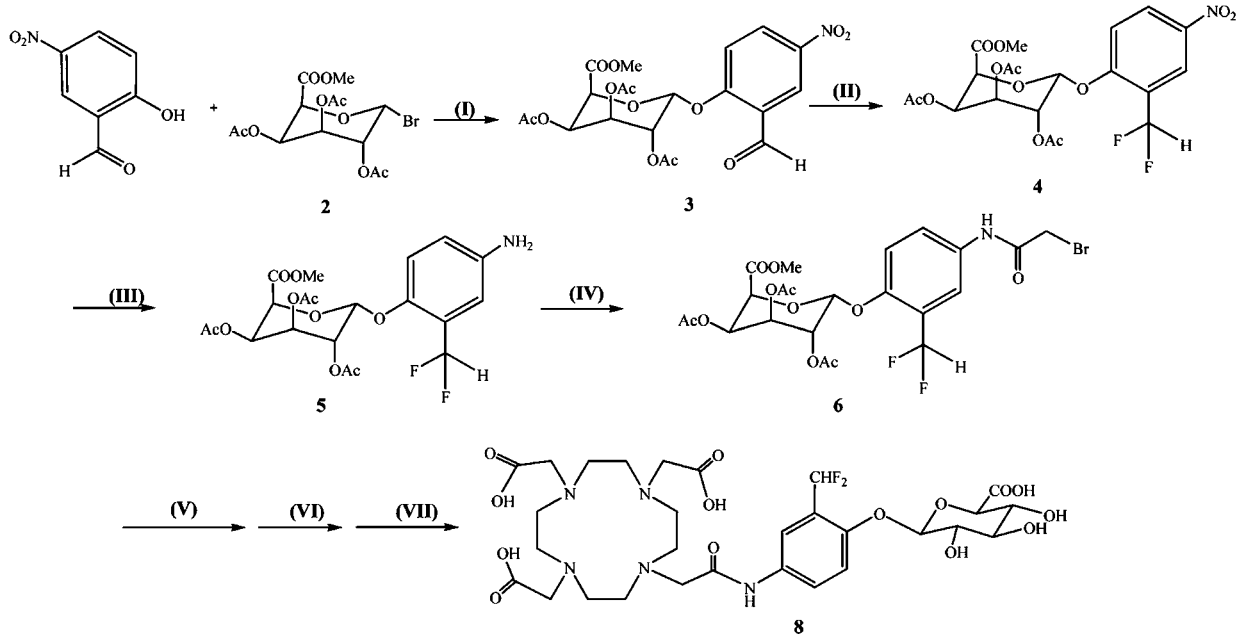

[a]Reagents and conditions: (I) Ag_2O, CH_3CN, 66%; (II) DAST, CH_2Cl_2, 88.4%; (III) H_2, Pd/C, CH_3CN, 94.3%; (IV) bromoacetyl bromide, K_2CO_3, CH_2Cl_2, 90.5%; (V) DO3A-tris-^{t}butyl ester (7), triethylamine, CH_3CN; (VI) $NaOCH_3$, CH_3OH; (VII) 1 N NaOH, 13% for three steps.

1. INTRODUCTION

Advancement in the molecular biology of cancer has drawn the attention of the radiological community to devise innovative methods that can facilitate noninvasive visualization of expression of cancer-related genes. Over the past two decades targeted magnetic resonance imaging (MRI) contrast agents have been extensively explored to accomplish the above objective.[1−6] However, many useful targets that are associated with disease states are present at nanomolar concentrations. Therefore, it is extremely difficult to develop disease-specific MRI contrast agents. In the late 1990s, a new class of MRI contrast agent, the so-called "smart" contrast agent, was introduced. The basic idea of smart contrast agents is the activation of silent inactive contrast agents in response to specific biological activity. The approach was experimentally demonstrated by β-galactosidase responsive Gd(III) based MRI contrast agent, (4,7,10-tri(acetic acid)-l-(2-β galactopyranosylethoxy)-1,4,7,10-tetraazacyc1ododecane) gadolinium (EGad).[7] A galactopyranose residue was conjugated at the ninth coordination site of the Gd(III) ion, thus blocking the entry of water molecules to an open coordination site. The galactopyranose moiety acts as substrate for β-galactosidase which upon enzymatic removal opens the access of water molecules to the paramagnetic center and thereby shortening the relaxation time of water proton. A successive attempt was made to evaluate potential applications of this new class of contrast agent for *in vivo* application using (1-(2-(β-galactopyranosyloxy)-propyl)-4,7,10-tris(carboxymethyl)-1,4,7,10-tetraazacyclododecane)-gadolinium(III) (EgadMe). Unfortunately, the study showed a moderate difference of 20% in the relaxivity of EgadMe before and after exposure to β-galactosidase, which was inadequate for robust *in vivo* MR imaging.[8] A novel pro-receptor-induced magnetization enhancement (pro-RIME) approach was followed by Hanaoka et al. and Nivorozhkin et al. to develop β-galactosidase[9] and human carboxypeptidase B[10] responsive pro-RIME MRI contrast agents. The approach relies upon enzymatic removal of a structural moiety that prevents binding of pro-RIME Gd(III) complex to human serum albumin (HSA). Binding of Gd(III) complex to HSA slows down the molecular rotation of the Gd(III) complex resulting in an additional increase in the relaxivity. Similarly, we developed a Gd(III) based contrast agent for *in vivo* visualization of β-galactosidase in tumor.[11] The difference in T_1 relaxivity in the absence and presence of β-galactosidase was adequate for robust *in vivo* imaging of β-galactosidase activity in the tumor tissues. Bodganov et al. reported tyrosinase- or myeloperoxidase-activated conversion of Gd(III) complex monomer into oligomer/polymer which further increased relaxivity of the contrast agents.[12] More recently, Aime et al. described β-galactosidase-activated conversion of Gd(III) monomer into oligomer/polymer.[13] Overall this strategy seems successful for developing contrast agents for enzyme activity profiling.

Studies have shown that tumors contain relatively higher concentration of lysosomal enzymes as compared to normal tissue.[14−16] The β-glucuronidase is a key marker enzyme for lysosomal activity.[17,18] Elevated β-glucuronidase activity has been observed in the breast, head, neck, and pancreatic cancer.[19,20] In addition, high levels of β-glucuronidase can be found in homogenates of human gastric tumor tissues and in several body fluids associated with various tumors.[21] Therefore, MRI contrast agents that can facilitate noninvasive visualization of β-glucuronidase are of great importance to detect β-glucuronidase-overexpressing tumors. In this study, we designed and synthesized (Scheme 1) a new β-glucuronidase activity-dependent pro-RIME contrast agent, [Gd(DOTA-FPβGu)] (DOTA-FPβGu = 1-(2-difluoromethyl-4-(1-(4,7,10-triscarboxymethyl (1,4,7,10-tetraazacyclodecyl))-acetamido)phenyl)-β-D-glucopyronuronate), for noninvasive visualization of β-glucuronidase expression in the tumor tissues. [Gd(DOTA-FPβGu)] consists of a Gd(III) complex and a β-glucuronidase-specific substrate (β-D-glucopyranuronic acid). The binding affinity of [Gd(DOTA-FPβGu)] toward HSA was assessed by proton relaxation enhancement (PRE) methods to evaluate of pro-RIME nature of [Gd(DOTA-FPβGu)]. We postulated that the

dx.doi.org/10.1021/ic301827p | *Inorg. Chem.* 2012, 51, 12426−12435

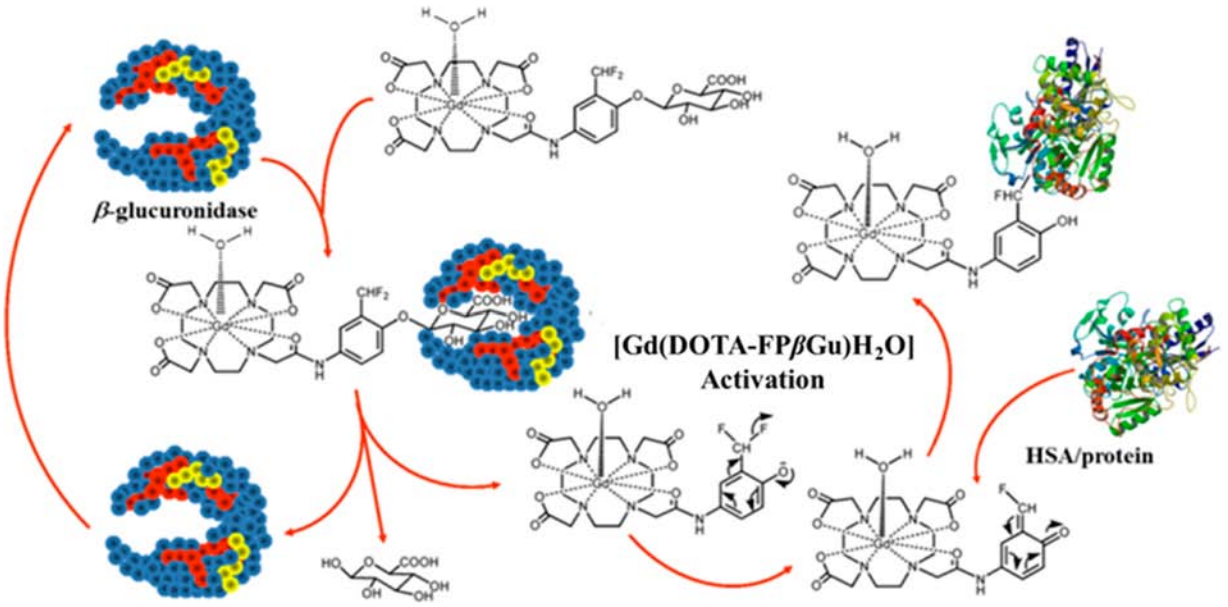

Figure 1. Systematic representation of β-glucuronidase induced transformation of pro-RIME [Gd(DOTA-FPβGu)] into ([Gd(DOTA-FP)]-HSA).

β-D-glucopyranuronic acid moiety of [Gd(DOTA-FPβGu)] would be specifically recognized and cleaved by β-glucuronidase. Enzymatic removal of β-glucuronic acid followed by nucleophile attack from HSA would eventually lead to the formation of stable high molecular weight biomacromolecule ([Gd(DOTA-FP)]-HSA) (Figure 1). Detailed mechanism of enzymatic activation of [Gd(DOTA-FPβGu)] was investigated by LC-MS. In addition, enzyme kinetic study was carried out to evaluate β-glucuronidase affinity for [Gd(DOTA-FPβGu)]. Longitudinal relaxation time (T_1) was investigated after incubation with β-glucuronidase. Finally, *in vivo* MR image of BALB/c mice bearing subcutaneous tumor xenografts with varying expression levels of β-glucuronidase was performed after tail vein intravenous injection of [Gd(DOTA-FPβGu)].

2. EXPERIMENTAL SECTION

2.1. Materials. Unless otherwise stated, all reagents were purchased from commercial suppliers and used without further purification. 2-Hydroxy-5-nitrobenzaldehyde, silver(I) oxide, and diethylaminosulphur trifluoride (DAST) were obtained from Alfa Aesar. HSA (product number A-1653, Fraction V Powder 96−99%) and β-glucuronidase (product number G7396-5KU, Type IX-A from *Escherichia coli*) were purchased from Sigma-Aldrich. The molecular weights of HSA and β-glucuronidase were assumed to be 66.9 and 290 kDa, respectively. Methyl 1-bromo-2,3,4-tri-*O*-acetyl-α-D-glucopyronuronate[22] and 4,7,10-(tris-^{t}butylcarboxymethyl)-(1,4,7,10-tetraazacyclodecane) (DO3A-tris-^{t}butyl ester) were prepared as previously published.[23,24] ^{1}H (400 MHz) and ^{13}C (100 MHz) NMR spectra were recorded on a Varian Gemini-400 spectrometer with 5 mm sample tubes. The ^{13}C NMR spectra were referenced internally relative to 3-(trimethylsilyl)-1-propanesulfonic acid for D_2O. The concentration of Gd(III) complex was determined by ICP-AES with a Perkin-Elmer OPTIMA 2000.

*2.1.1. Synthesis. 2.1.1.1. Methyl 1-(2-Formyl-4-nitrophenyl)-2,3,4-triacetyl-β-D-glucopyronuronate (**3**).* To a solution of 1-bromo-2,3,4-tri-*O*-acetyl-α-D-glucopyronuronate (26.8 g, 67.5 mmol) in anhydrous acetonitrile (200 mL) was added 2-hydroxy-5-nitrobenzaldehyde (12.4 g, 74.3 mmol) and silver(I) oxide (31.4 g, 135 mmol). The mixture solution was stirred in the dark at 0 °C for 4 h. The crude reaction mixture was filtered to remove solids, and the filtrate was concentrated under reduced pressure. The red oil was extracted with ethyl acetate (2 × 400 mL). The combined ethyl acetate extracts were washed with sodium bicarbonate (3 × 200 mL), water, and brine and dried over magnesium sulfate anhydrous. After filtration, the solvent was removed under reduced pressure, and the residue thus obtained was purified by silica gel column chromatography (50% ethyl acetate in hexane) to give the product as a white powder (21.5 g, 66%). ^{1}H NMR (400 MHz, $CDCl_3$): δ 2.08 (s, 9H, OAc), 3.73 (s, 3H, $COOCH_3$), 4.33 (m, 1H, sugar, CH), 5.41 (m, 4H, sugar, CH), 7.29 (s, 1H, ArH), 8.44 (dd, 1H, ArH), 8.72 (d, 1H, ArH), 10.33 (s, 1H, CHO). ^{13}C NMR (100 MHz, $CDCl_3$): δ 20.47, 20.53, 20.55, 53.19, 68.46, 70.27, 71.67, 72.73, 97.90, 115.89, 124.43, 125.81, 130.28, 143.43, 161.77, 166.37, 169.06, 169.26, 169.79, 186.76. ESI-MS: calcd m/z 483.4, found 484.7 $[M + H]^+$. Anal. Calcd for $C_{20}H_{21}NO_{13}$: C 49.69, H 4.38, N 2.90. Found: C 49.91, H 4.56, N 3.07.

*2.1.1.2. 1-(2-Difluoromethyl-4-nitrophenyl)-2,3,4-triacetyl-β-D-glucopyronuronate (**4**).* To a solution of methyl 1-(2-formyl-4-nitrophenyl)-2,3,4-triacetyl-β-D-glucopyronuronate (7.50 g, 15.5 mmol) in anhydrous dichloromethane (300 mL) was added DAST (2.44 mL, 18.6 mmol). The mixture solution was stirred at room temperature under N_2 for 8 h. The reaction was quenched by the addition of ice. The reaction mixture was washed with water and brine and dried over magnesium sulfate anhydrous. After filtration, the solvent was removed under reduced pressure, and the yellow residue thus obtained was purified by silica gel column chromatography (100% dichloromethane) to give the product as a white powder (6.93 g, 88.4%). ^{1}H NMR (400 MHz, $CDCl_3$): δ 2.07 (s, 9H, OAc), 3.74 (s, 3H, $COOCH_3$), 4.31 (m, 1H, sugar, CH), 5.31 (dd, 1H, sugar, CH), 5.36 (m, 3H, sugar, CH), 6.83 (t, 1H, CHF_2), 7.24 (d, 1H, ArH), 8.36 (dd, 1H, ArH), 8.49 (t, 1H, ArH). ^{13}C NMR (100 MHz, $CDCl_3$): δ 20.36, 20.37, 20.46, 20.51, 53.17, 68.59, 69.94, 70.70, 72.69, 98.39, 107.55, 109.93, 112.30, 122.70, 122.75, 122.79, 122.83, 127.83, 143.18, 158.39, 166.36, 169.22, 169.25, 169.81. ESI-MS: calcd m/z 505.4, found 506.3 $[M + H]^+$. Anal. Calcd for $C_{20}H_{21}F_2NO_{12}$: C 47.53, H 4.19, N 2.77. Found: C 47.88, H 4.16, N 3.08.

*2.1.1.3. 1-(2-Difluoromethyl-4-aminophenyl)-2,3,4-triacetyl-β-D-glucopyronuronate (**5**).* To a solution of 1-(2-difluoromethyl-4-nitrophenyl)-2,3,4-triacetyl-β-D-glucopyronuronate (3.90 g, 7.70 mmol) in acetonitrile (50 mL) was added Pd/C (10% Pd, 77 mg). The mixture was stirred at room temperature under 1.8 atm H_2. This step was repeated until the pressure stopped decreasing. After pressure reached stabilization the mixture was filtered, and the solvent was removed under reduced pressure. The yellow residue thus obtained was purified by silica gel column chromatography (66% ethyl acetate in hexane) to give the product as a yellow powder (3.45 g, 94.3%). ^{1}H NMR (400 MHz, $CDCl_3$): δ 2.05 (s, 6H, OAc), 2.07 (s, 3H, OAc), 3.76 (s, 3H, $COOCH_3$), 4.14 (d, 1H, sugar, CH), 4.96 (d, 1H, sugar, CH), 5.31 (m, 3H, sugar, CH), 6.71 (dd, 1H, ArH), 6.78 (t, 1H, CHF_2), 6.86 (q, 1H, ArH), 6.95 (d, 1H, ArH). ^{13}C NMR (100 MHz, $CDCl_3$): δ 20.42, 20.45, 20.54, 52.99, 69.12,

70.58, 71.63, 72.46, 100.54, 108.78, 111.13, 112.09, 112.13, 112.17, 112.20, 113.48, 118.07, 118.18, 142.84, 142.83, 166.75, 169.36, 170.02. ESI-MS: calcd m/z 475.4, found 476.8 $[M + H]^+$. Anal. Calcd for $C_{20}H_{23}F_2NO_{10}$: C 50.53, H 4.88, N 2.95. Found: C 50.59, H 5.16, N 2.84.

*2.1.1.4. 1-(2-Difluoromethyl-4-(1-bromoacetamido)phenyl)-2,3,4-triacetyl-β-D-glucopyronuronate (**6**).* To a solution of 1-(2-difluoromethyl-4-(1-bromoacetamido) phenyl)-2,3,4-triacetyl-β-D-glucopyronuronate (2.50 g, 5.26 mmol) in anhydrous dichloromethane (50 mL) was added potassium carbonate (0.87 g, 6.31 mmol), and the solution was cooled in ice bath with stirring. Bromoacetyl bromide (1.59 g, 7.89 mmol) was added dropwise into the stirred reaction mixture on ice bath overnight. The crude reaction mixture was filtered and washed with saturated sodium bicarbonate (3 × 200 mL), water, and brine and dried over anhydrous magnesium sulfate. After filtration, the solvent was removed under reduced pressure, and the residue thus obtained was purified by silica gel column chromatography (17% ethyl acetate in dichloromethane) to give the product as yellow powder (2.84 g, 90.5%). ^{1}H NMR (400 MHz, $CDCl_3$): δ 2.06 (s, 9H, OAc), 3.76 (s, 3H, $COOCH_3$), 4.02 (s, 2H, CH_2Br), 4.22 (dd, 1H, sugar, CH), 5.10 (d, 1H, sugar, CH), 5.34 (m, 3H, sugar, CH), 6.81 (t, 1H, CHF_2), 7.11 (d, 1H, ArH), 7.58 (d, 1H, ArH), 7.77 (dd, 1H, ArH), 8.25 (s, 1H, NH). ^{13}C NMR (100 MHz, $CDCl_3$): δ 20.41, 20.47, 20.54, 53.08, 68.96, 70.33, 71.35, 72.49, 99.51, 108.33, 110.68, 113.04, 116.52, 118.24, 118.28, 118.32, 118.36, 124.07, 132.79, 132.81, 163.63, 166.62, 169.35, 169.97. ESI-MS: calcd m/z 596.3, found 597.1 $[M + H]^+$. Anal. Calcd for $C_{22}H_{24}BrF_2NO_{11}$: C 44.31, H 4.06, N 2.35. Found: C 44.42, H 4.14, N 2.49.

*2.1.1.5. 1-(2-Difluoromethyl-4-(1-(4,7,10-triscarboxymethyl-(1,4,7,10-tetraazacyclodecyl)) acetamido)phenyl)-β-D-glucopyronuronate (DOTA-FPβGu, **8**).* To a solution of DO3A-tris-^{t}butyl ester (1.87 g, 2.04 mmol) in acetonitrile (50 mL) was added triethylamine (0.55 mL, 3.93 mmol) and 1-(2-difluoromethyl-4-(1-bromoacetamido)-phenyl)-2,3,4-triacetyl-β-D-glucopyronuronate (1.18 g, 1.93 mmol). The mixture was heated to 70 °C and stirred for 24 h. After filtration solvent was evaporated under reduced pressure. The acetyl group was removed by reaction with sodium methoxide and dry methanol (50 mL) for 2 h. Deprotections of tert-butyl ester groups and methyl groups were achieved by stirring at ice bath in 1 N sodium hydroxide solution (20 mL) for 8 h. This compound was purified by AG 1 × 8 anion exchange resin column (200−400 mesh, HCO_2^- form, eluted first with H_2O and then with a gradient of formic acid) and then collected and concentrated by 0.12−0.15 N formic acid solution. The trace of formic acid was removed by coevaporation with water (3 × 100 mL), and freeze-dried to give a white powder (0.37 g, 13.0%). ^{1}H NMR (400 MHz, $CDCl_3$): δ 3.06 (m, 8H, DOTA, N−CH_2CH_2−N), 3.30 (m, 8H, DOTA, N−CH_2CH_2−N), 3.55 (m, 6H, DOTA, N−CH_2COOH), 3.75 (m, 5H, sugar and DOTA, CH and N−CH_2-CO), 4.00 (d, 1H, sugar, CH), 5.07 (d, 1H, sugar, −CH−), 7.00 (t, 1H, −CHF_2), 7.15 (d, 1H, ArH), 7.43 (dd, 1H, ArH), 7.61 (s, 1H, ArH). ^{13}C NMR (100 MHz, $CDCl_3$): δ 48.85, 51.06, 55.35, 55.74, 59.94, 71.42, 72.66, 75.19, 75.28, 100.78, 104.72, 114.45, 116.80, 119.11, 123.97, 125.37, 132.59, 162.61, 172.96. ESI-MS: calcd m/z 721.7, found 722.2 $[M + H]^+$. Anal. Calcd for $C_{29}H_{41}F_2N_5O_{14}$: C 48.27, H 5.73, N 9.70. Found: C 48.35, H 5.84, N 9.75. The purity of DOTA-FPβGu was determined by HPLC and mass. The HPLC chromatogram has been deposited as Supporting Information (Figure S1)

2.1.2. Preparation of Lanthanide Complexes. The Gd(III) and Eu(III) complexes were prepared by dissolving the DOTA-FPβGu (0.42 g, 0.58 mmol) in H_2O (10 mL) and adjusting the pH of the solution to 6.5 with dilute sodium hydroxide. $LnCl_3$ (0.57 mmol, dissolved in 5 mL H_2O and brought to pH = 6.5 with sodium hydroxide) was added dropwise, maintaining pH at 5.5−6.5 with dilute sodium hydroxide periodically. The mixture solution was stirred over an ice bath for 1 day, the pH was maintained, and the formation of Ln(III) chelate was considered complete. The pH was brought to 8.0, and the solution was centrifuged to remove excess lanthanide ions as $Ln(OH)_3$ and verified by the xylenol orange test. The trace $Ln(OH)_3$ was removed by filtrating with 200 nm nylon filter, and the solution was freeze-dried under reduced pressure. The purity of [Gd(DOTA-FPβGu)] was determined by HPLC and mass. The HPLC chromatogram has been deposited as Supporting Information (Figure S2)

2.2. Methods. *2.2.1. Reversed Phase High-Performance Liquid Chromatography (HPLC) Method.* The HPLC experiments were performed on an Amersham ÄKTAbasic 10 equipped with an Amersham UV-900 detector and Amersham Frac-920 fraction collector. A Supelcosil RP-C18 column (5 μm, 4.6 mm × 250 mm) was used.

2.2.2. Relaxation Time Measurement. The longitudinal relaxation times (T_1) of Gd(III) complex were measured to determine relaxivity (r_1). The measurements were made using a relaxometer operating at 20 MHz and 37.0 ± 0.1 °C (NMR-120 minispec, Bruker). Before each measurement the relaxometer was tuned and calibrated. The values of r_1 were determined from 5 data points generated by an inversion−recovery pulse sequence. To study the effect of β-glucuronidase cleavage of β-D-glucopyranuronic acid on the T_1 value of [Gd(DOTA-FPβGu)] solutions, β-glucuronidase isolated from *Escherichia coli* was used. The *Escherichia coli* enzyme was reconstituted with 0.1 M sodium phosphate buffer solution (PBS), pH = 7.4 at 25.0 ± 0.1 °C. For the longitudinal relaxation time (T_1) measurements of [Gd(DOTA-FPβGu)] in the presence or absence of β-glucuronidase and HSA, the follow reactions were set up: (a) 0.5 mM [Gd(DOTA-FPβGu))] in 100 mM PBS; (b) 0.5 mM [Gd(DOTA-FPβGu)] and 0.1 mg/mL β-glucuronidase in 100 mM PBS; (c) 0.5 mM [Gd(DOTA-FPβGu)] and 0.5 mM HSA in 100 mM PBS; (d) 0.5 mM [Gd(DOTA-FPβGu)], 0.5 mM HSA, and 0.01 mg/mL β-glucuronidase in 100 mM PBS; (e) 0.5 mM [Gd(DOTA-FPβGu)], 0.5 mM HSA, and 0.1 mg/mL β-glucuronidase in 100 mM PBS. The percentage change of T_1 value in these solutions was plotted against the incubation time. These measurements were made in triplicate to reduce systematic error in the relaxation time (T_1) measurements.

2.2.3. Enzyme Kinetics. All reactions were performed in a quartz cell at 37.0 ± 0.1 °C. The final reaction mixture had a volume of 3.0 mL containing [Eu(DOTA-FPβGu)] (0.25, 0.5, 1.0, 2.0, 4.0, and 6.0 mM) in 100 mM PBS (pH 7.4 ± 0.1). Luminescence intensity at 616 nm (excitation λ_{max} = 318 nm) was measured after addition of the β-glucuronidase (0.1 mg/mL) to initiate the enzymatic reaction and was recorded every 30 s continuously by a Varian Cary Eclipse fluorescence spectrophotometer. The initial velocity for each enzymatic reaction in the presence of a specific [Eu(DOTA-FPβGu)] concentration was obtained by determining the slope of the change of luminescence within the first 3 min of the reaction. Acquired initial velocity for each concentration of [Eu(DOTA-FPβGu)] was plotted to fit the data into the Michaelis−Menten equation $[v = (V_{max}[\text{Eu(DOTA-FP}\beta\text{Gu)}])/(K_M + [\text{Eu(DOTA-FP}\beta\text{Gu)}])]$ and obtain K_M, k_{cat}, and k_{cat}/K_M.

2.2.4. Butanol Buffer Partition Coefficient. [Gd(DOTA-FPβGu)] (0.07 mM) in 10 mL of PBS was equilibrated at room temperature for 1−2 h with PBS-saturated butanol (10 mL). The vials were centrifuged at 2000 *g* for 5 min to ensure that the layers were separated. Aliquots (5 mL) from each phase were removed and analyzed via inductively coupled plasma−atomic emission spectroscopy (ICP-AES, PerkinElmer OPTIMA 2000 PV). The partition coefficient (P) was calculated by eq 1[25−27]

$$P = \frac{\text{avg conc of Gd(III) complex in butanol}}{\text{avg conc of Gd(III) complex in PBS}} \quad (1)$$

2.2.5. Cells and Animals. CT26 and CT26/mβG-eB7 (Supporting Information S1)[28] murine colon carcinoma cells were grown in Dulbecco's minimal essential medium (DMEM) supplemented with 5% bovine calf serum and 100 U/mL penicillin, 100 μg/mL streptomycin (Sigma) in a humidified 37.0 ± 0.1 °C, 5% CO_2 atmosphere.

Eight-week-old Balb/c mice were purchased from the National Laboratory Animal Center of Taiwan (Taipei, Taiwan). All animal experiments were performed in accordance with institute guidelines. 2 ×10^6 CT26/mβG-eB7 and 2 × 10^6 CT26 tumor cells were injected subcutaneous to right and left hind limb, respectively. Whole body image was performed a MR imaging scanner (Sigma; GE Medical Systems) two to three weeks after the injection when tumors grew to a diameter of 5−10 mm.

2.2.6. MR Imaging Studies of Enzymatic Activation of [Gd(DOTA-FPβGu)]. Four reactions were set up to study the MR images of [Gd(DOTA-FPβGu)] and its β-glucuronidase-cleavaged product: (a) 0.5 mM [Gd(DOTA-FPβGu)] in 100 mM PBS (pH = 7.4), (b) 0.5 mM [Gd(DOTA-FPβGu)] and 0.5 mM HSA in 100 mM PBS (pH = 7.4),

(c) 0.5 mM [Gd(DOTA-FPβGu)], 0.1 mg/mL β-glucuronidase, and 0.5 mM HSA in 100 mM PBS (pH = 7.4), and (d) 100 mM PBS (pH = 7.4). The solutions were transferred to 1.5-mL test tubes for MR imaging. MR imaging was performed with a clinical 3.0 T magnetic resonance scanner and a knee coil. MR pulse sequence included T_1-weighted (TR/TE 100/10 ms) two-dimensional spin−echo sequence. Mean signal intensities (SIs) for the test tubes were measured in the central section of the imaging volume with use of operator-defined regions of interest with a minimum of 10 pixels per region. To compare differences in SI data between various test tubes, analysis of variance for repeated measurements was used. Mean data were compared with the Scheffe test. A P value of less than 0.05 was considered to indicate a statistically significant difference.

2.2.7. In Vitro MR Imaging Studies of [Gd(DOTA-FPβGu)]. In vitro MR imaging studies were performed with a clinical 3.0 T magnetic resonance scanner and a knee coil. CT26/mβG-eB7 and CT26 cells (2×10^6) were incubated [Gd(DOTA-FPβGu)] (1 mM Gd in 1 mL medium) at 37.0 ± 0.1 °C for 30 min. Cells were scanned by a fast gradient echo pulse sequence (TR/TE/flip angle = 100/5.8/10). The enhancement (%) was calculated by eq 2[29]

$$\text{enhancement (\%)} = \frac{\text{SI}_{\text{post}} - \text{SI}_{\text{pre}}}{\text{SI}_{\text{pre}}} \times 100 \quad (2)$$

where SI_{pre} is the signal intensity for cells untreated with the contrast agent and SI_{post} is the signal intensity for cells treated with the contrast agents

2.2.8. In Vivo MR Imaging. Twelve BALB/c mice bearing established CT26 and CT26/mβG-eB7 tumors (200−300 mm^3) in left and right leg regions, respectively, were anesthetized with 80 mg/kg ketamine and 8 mg/kg xylazine, and then each mouse was placed in an animal coil in prone position. MR imaging was performed using a 3T MR scanner. T_1-weighted FSE (TR/TE 100/15 ms) axial images before injection of the contrast agents were obtained. After preinjection scanning, six mice were intravenously injected with 0.1 mmol/kg [Gd(DOTA-FPβGu)] from tail vein; the other six mice were intravenously injected with 0.1 mmol/kg $[\text{Gd(DTPA)}]^{2-}$. Postcontrast scans were obtained every 5 min for six subsequent scans, and then scanned every 5 min until 90 min. A glass cylinder containing pure water as a reference standard was positioned adjacent to each mouse.

2.2.9. Histological Analysis. After MR imaging, tumors were excised and embedded in O.C.T compound (Tissue-Tek) (Sakura Finetek, Torrance) at −80 °C, and then tumors were sectioned into 10 μm slices, stained for β-glucuronidase activity with the β-glucuronidase reported gene staining kit (Sigma Diagnostics), and counterstained with nuclear fast red. Each section was examined on an upright BX4 microscopy (Olympus) or viewed in phase contrast and fluorescent modes on an inverted Axiovert 200 microscope (Carl Zeiss Microimaging).

2.2.10. Cytotoxicity of [Gd(DOTA-FPβGu)]. CT-26 and CT26/mβG-eB7 cells were seeded overnight in 96-well plates. Gradient concentrations (1 mM to 5 μM) of [Gd(DOTA-FPβGu)] were added into CT-26 and CT26/mβG-eB7 cells in triplicate for overnight, the medium was refreshed, and the sample was subsequently incubated an additional 48 h at 37.0 ± 0.1 °C. Cell viability was determined by the ATPlite luminescence ATP detection assay system (Perkin-Elmer Life and Analytical Science). Results are expressed as percent inhibition of luminescence as compared to untreated cells by eq 3

$$\text{inhibition \%} = \frac{\text{sample luminescence}}{\text{control luminescence}} \times 100 \quad (3)$$

where control luminescence is the background luminescence.

2.2.11. Image Analysis. The regions of interest (ROI) from image of the tumors and the water phantom were selected by the researchers. The position of ROI must be chosen to avoid incorrect signal. The signal intensity (SI) of each tumor was normalized by dividing its mean target signal intensity by that of the water phantom (signal-to-noise ratio, SI/N). The enhancement percentage of the targets was calculated by eq 4

$$\text{enhancement (\%)} = \frac{\left(\frac{\text{SI}}{N}\right)\text{t} - \left(\frac{\text{SI}}{N}\right)\text{pre}}{\left(\frac{\text{SI}}{N}\right)\text{pre}} \times 100 \quad (4)$$

where (SI/N)t and (SI/N)pre were the SI/N of the targets at postcontrast and precontrast, respectively. Enhancement percentages at different time points were compared between different groups. The results were calculated and expressed as the mean ± SD. Statistics were performed with statistical softwares (JMP 8, SAS Institute Inc., Cary, NC; Prism, GraphPad software Inc.). Two-way analysis of variance (ANOVA) using random effect model was used to compare the different groups. Posthoc comparison for enhancement at each time point was also carried out when significant difference occurred. P-values of less than 0.05 were considered statistically significant.

3. RESULTS AND DISCUSSION

3.1. Synthesis of the Ligand. The ligand DOTA-FPβGu was synthesized in seven steps, as shown in Scheme 1. Methyl 1-(2-formyl-4-nitrophenyl)-2,3,4-triacetyl-β-D-glucopyronuronate (**3**) was synthesized via alkylation-coupling reactions between 2-hydroxy-5-nitrobenzaldehyde and 1-bromo-2,3,4-tri-*O*-acetyl-α-D-glucopyronuronate in the presence of silver(I) oxide. The duration of reaction was critically monitored to avoid decomposition of glucopyronuronate. Subsequently, aldehyde was fluorinated and nitro group was hydrogenated to the amino group. The bromoacetyl group was used as a linker to bind DO3A-tris-^{t}butyl ester and 2-difluoromethylphenyl-β-D-glucopyronuronate. Finally, hydrolysis was carried out to obtain DOTA-FPβGu, which was achieved in two steps. First, the acetyl group in glucopyronuronate was hydrolyzed with sodium methoxide, and second, methyl esters in glucopyronuronate and tert-butyl groups in DOTA were hydrolyzed by sodium hydroxide. The ligand, DOTA-FPβGu, was analyzed by HPLC (Figure S1 in the Supporting Information), which was identified by ESI-MS.

3.2. Activation Mechanism, Specificity, and Enzyme Kinetics. The postulated activation mechanism of [Gd(DOTA-FPβGu)] was experimentally validated using LC-MS technique. LC-MS provided a convenient means of detecting and identifying the components of the enzyme-catalyzed hydrolysis of [Gd(DOTA-FPβGu)]. In order to demonstrate [Gd(DOTA-FPβGu)] as a β-glucuronidase activated pro-RIME contrast agent, L-lysine was used as a substituent of HSA. Figure 2 shows the HPLC chromatograms of 0.5 mM [Gd(DOTA-FPβGu)] in the presence of 0.1 mg/mL β-glucuronidase (a), and 0.5 mM [Gd(DOTA-FPβGu)] in the presence of 0.1 mg/mL β-glucuronidase and excess L-lysine (b) in PBS buffer (pH 7.4). [Gd(DOTA-FPβGu)], [Gd(DOTA-FP)], and [Gd(DOTA-FP)]-L-lysine were detected in HPLC chromatograms as shown in Figure 2 at 5.2, 10.2, and 18.1 min, respectively. The molecular weights of different fragments were confirmed by LC-MS (ESI^+) [calculated m/z 875.8, found m/z: 876.5 $[M + H]^+$; calculated m/z 679.75, found m/z: 680.2 $[M + H]^+$; and calculated m/z 825.94, found m/z: 826.62 $[M + H]^+$, respectively]. These results indicate that [Gd(DOTA-FP)] can efficiently bind to HSA after digestion by β-glucuronidase.

Having established the activation mechanism of [Gd(DOTA-FPβGu), we then evaluated whether [Gd(DOTA-FPβGu)] is β-glucuronidase-specific. The selectivity of [Gd(DOTA-FPβGu) between β-glucuronidase and β-galactosidase is especially promising because the active sites of these two enzymes recognize similar chemical structures (Chart 1). Figure 3 shows HPLC chromatograms of [Gd(DOTA-FPβGu)] incubated with 0.1 mg/mL β-glucuronidase. Unlike HPLC chromatogram obtained in the presence of β-glucuronidase, no new peak was detected in the presence of β-galactosidase. From these two studies we can

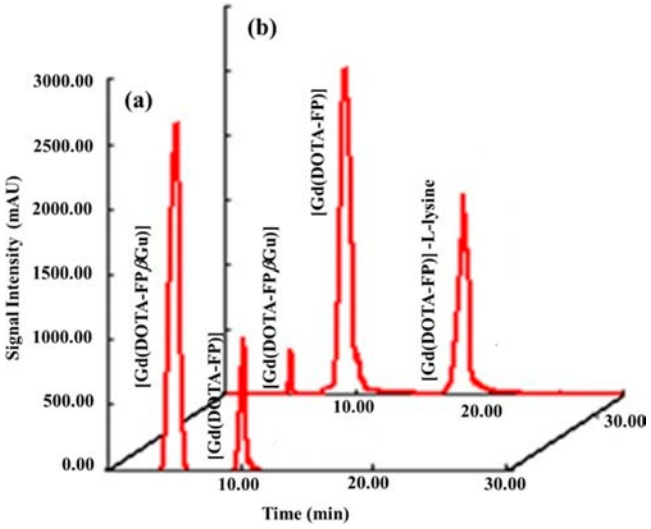

Figure 2. HPLC analysis of [Gd(DOTA-FPβGu)] incubated with β-glucuronidase: (a) 0.5 mM [Gd(DOTA-FPβGu)] in the presence of 0.1 mg/mL β-glucuronidase, and (b) 0.5 mM [Gd(DOTA-FPβGu)] in the presence of 0.1 mg/mL β-glucuronidase and excess L-lysine in pH 7.4 Tris buffer at 298 K. After incubation, samples were analyzed by HPLC using gradient of 100% to 0% water in CH_3OH as organic phase, flow rate 0.5 mL/min. Eluates were detected at 254 nm.

Chart 1

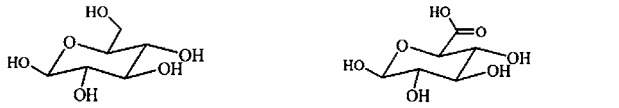

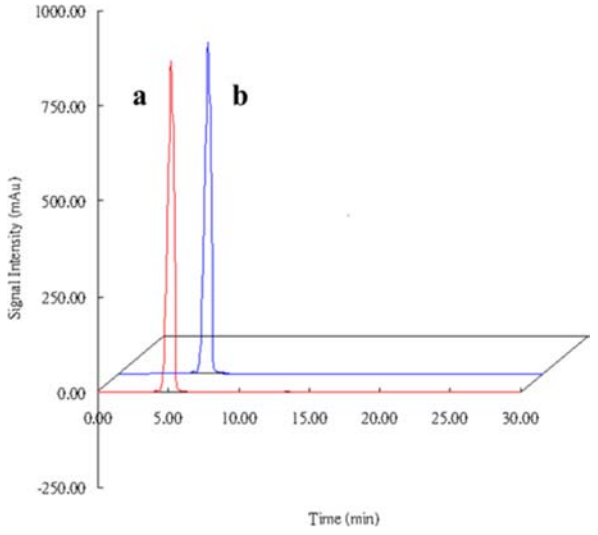

Figure 3. HPLC analysis of (a) [Gd(DOTA-FPβGu)] alone and (b) [Gd(DOTA-FPβGu)] incubated with β-galactosidase. Same experimental procedures were used as shown in Figure 2 except β-galactosidase was used.

conclude that [Gd(DOTA-FPβGu)] is specific for β-glucuronidase.

The kinetic parameters for the enzyme reaction of [Eu(DOTA-FPβGu)] with β-glucuronidase were determined by measuring the luminescence change of [Eu(DOTA-FPβGu)].[9] The kinetic parameters, K_m and k_{cat}, were determined by direct fitting of the initial velocity versus substrate concentration to the Michaelis–Menten equation as shown in Figure 4 and summarized in Table 1

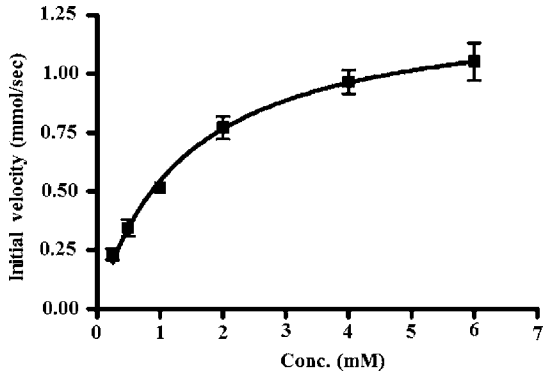

Figure 4. Kinetics of [Eu(DOTA-FPβGu)] hydrolysis catalyzed by bovine liver β-glucuronidase (1.0 mg/mL) in 100 mM sodium phosphate buffer, 0.01% (w/v) bovine serum albumin (BSA), pH = 7.4 at 37.0 ± 0.1 °C. Each point represents the average of three independent experiments ±1 standard deviation. Line represents best fit curve to Michaelis–Menten model.

along with the standard substrate 4-nitrophenyl-β-D-glucopyranoside (pNPG) as reference. The values of K_m, k_{cat}, and k_{cat}/K_m of [Eu(DOTA-FPβGu)] for β-glucuronidase were 1.38 mM, 3.76×10^3 s^{-1}, and 2.72×10^3 mM^{-1} s^{-1}, respectively. The K_m of [Eu(DOTA-FPβGu)] is significantly lower than that of pNPG for β-glucuronidase.[30] Consequently, lower concentration β-glucuronidase is required for activation of [Eu(DOTA-FPβGu)]. In addition, k_{cat}/K_m of [Eu(DOTA-FPβGu)] for β-glucuronidase is significantly higher than that of pPNG, reflecting higher affinity of β-glucuronidase to [Eu(DOTA-FPβGu)].

3.3. Relaxometric Studies of the Gd(III) Complexes. The efficiency of MR contrast agent is evaluated in terms of relaxivity, which represents the net increase in water proton longitudinal relaxation rate per millimolar concentration of the paramagnetic compound.[31] The longitudinal relaxivity (r_1) value of [Gd(DOTA-FPβGu)] determined at 20 MHz and 37 ± 0.1 °C is 3.90 ± 0.07 mM^{-1} s^{-1}, which is similar to those of [Gd(DOTA-FPG)],[14] $[Gd(DOTA)]^-$,[32] [Gd(HP-DO3A)] (HP-DO3A = 1,4,7,10-tetraazacyclododecane-1-(2-hydroxylpropyl)-4,7,10-triaceticacid),[33] and [Gd(DTPA)][2−34] (Table 2). However, the relaxivity of [Gd(DOTA-FPβGu)] slightly decreased in the presence of β-glucuronidase, indicating that β-D-glucopyranuronic acid residue was removed from [Gd(DOTA-FPβGu)] by β-glucuronidase. On the contrary, 2-fold increase in relaxivity was observed in the presence of HSA. This result prompted us to determine the binding constant (K_A) of [Gd(DOTA-FPβGu)] to HSA. The experimental procedure involves two distinct titrations, called E- and M-titration (Supporting Information S2 and S3), and results of E- and M-titrations for [Gd(DOTA-FPβGu)] in the presence of HSA have been deposited as Supporting Information (Figures S3 and S4). The K_A value of [Gd(DOTA-FPβGu)] is $(9.0 \pm 0.1) \times 10^2$ M^{-1}, which is significantly lower than that of MS-325 ($(3.0 \pm 0.2) \times 10^4$ M^{-1}). This finding was further supported by lipophilic profile of [Gd(DOTA-FPβGu)]. The lipophilic profile of [Gd(DOTA-FPβGu)] was evaluated by log P (logarithm of partition coefficient in n-octanol/water) value. The log P value can estimate the lipophilicity of a compound in a biological environment, and thus, it is directly related to the binding affinity of Gd(III) complexes to HSA. Because of

dx.doi.org/10.1021/ic301827p | Inorg. Chem. 2012, 51, 12426–12435

Table 1. Enzyme Kinetic Parameter for [Eu(DOTA-FPβGu)] and *p*NPG

substrate	pH[a]	K_m (mM)	k_{cat}	k_{cat}/K_m (M^{-1} s^{-1})
[Eu(DOTA-FPβGu)][a]	7.4	1.38 ± 0.33	3.76 ± 0.58 × 10^3	2.72 ± 0.38 × 10^3
*p*NPG[b]	7.4	18.5 ± 5.6	1.25 × 10^2	6.76 ± 2.05

[a]With 1.0 mg/mL of bovine liver β-glucuronidase (type B-1), 100 mM sodium phosphate, 0.01% (w/v) bovine serum albumin (BSA). Data are average of three independent experiments ±1 standard deviation. [b]Data were obtained from ref 30.

Table 2. Relaxivity (r_1) of [Gd(DOTA-FPβGu)], [Gd(DOTA-FPβGu)] + βG, [Gd(DOTA-FPβGu)] + HSA, [Gd(DOTA-FPβGu)] + βG + HSA, [Gd(DOTA-FPG)], [Gd(DOTA)]$^-$, [Gd(HP-DO3A)], and [Gd(DTPA)]$^{2-}$ in 100 mM PBS at 37.0 ± 0.1 °C and 20 MHz

complex	pH	relaxivity (r_1/mM^{-1} s^{-1})
[Gd(DOTA-FPβGu)]	7.4 ± 0.1	3.90 ± 0.02
[Gd(DOTA-FPβGu)] + βG[a]	7.4 ± 0.1	3.68 ± 0.06
[Gd(DOTA-FPβGu)] + HSA[b]	7.4 ± 0.1	7.76 ± 0.05
[Gd(DOTA-FPβGu)] + βG + HSA[c]	7.4 ± 0.1	14.3 ± 0.3
[Gd(DOTA-FPG)][d]	7.4 ± 0.1	3.96 ± 0.04
[Gd(DOTA)]$^-$[e]	7.3 ± 0.1	3.56
[Gd(HP-DO3A)][f]	7.5 ± 0.1	3.65
[Gd(DTPA)]$^{2-}$[g]	7.6 ± 0.1	3.89 ± 0.03

[a][Gd(DOTA-FPβGu)] in the presence of β-glucuronidase (2 μM). [b][Gd(DOTA-FPβGu)] in the presence of HSA (0.5 mM). [c][Gd(DOTA-FPGu)] in the presence of β-glucuronidase (2 μM) and HSA (0.5 mM). [d]Data obtained from ref 11. [e]Reference 32. [f]Reference 33. [g]Reference 34.

the hydrophilic nature of the pro-RIME [Gd(DOTA-FPβGu)], partition coefficients were measured in butanol/PBS instead of octanol/PBS. The partition coefficient of the [Gd(DOTA-FPβGu)] in butanol/water (PBS buffer) was determined following previously reported method.[25,26] The log *P* value of [Gd(DOTA-FPβGu)] is −2.84 ± 0.15 which is comparatively lower than that of MS-325 (−2.11 ± 0.06).[27] This is reflected in the lower binding constant (K_A) (9.0 ± 0.1 × 10^2 M^{-1}) of [Gd(DOTA-FPβGu)] to HSA. The relaxivity of [Gd(DOTA-FPβGu)] in the presence of HSA and β-glucuronidase is about 4-fold higher than that of [Gd(DOTA-FPβGu)], suggesting that the enzymatic removal of pendent sugar moiety is accompanied by nucleophile attacks that lead to the formation of stable macromolecular adducts.

To evaluate [Gd(DOTA-FPβGu)] as a potential β-glucuronidase activated RIME contrast agent, a series of time-dependent experiments was conducted to evaluate change in the longitudinal relaxation time (T_1) in real time, and the results are shown in Figure 5. The longitudinal relaxation time (T_1) of [Gd(DOTA-FPβGu)] was investigated at different incubation time in the absence or presence of β-glucuronidase and HSA. The change in T_1 value of [Gd(DOTA-FPβGu)] in the PBS was not observed over a period of 60 min, reflecting stability of [Gd(DOTA-FPβGu)] under physiological pH. The T_1 of [Gd(DOTA-FPβGu)] increases by 8% in the presence of 0.1 mg/mL β-glucuronidase (Figure 5). This result is consistent with relaxometric study, and the anomalies in T_1 value can be explained by taking into account the change in molecular weight of [Gd(DOTA-FPβGu)]. Upon enzymatic cleavage, a significant amount of [Gd(DOTA-FP)] (relatively low molecular weight) was produced, and just a small fraction of [Gd(DOTA-FP)] strongly interacts with β-glucuronidase to form [Gd(DOTA-FP)]-β-glucuronidase adduct due to low concentration of β-glucuronidase (0.1 mg/mL). Therefore, an increase in relaxation time was observed after β-glucuronidase treatment. As

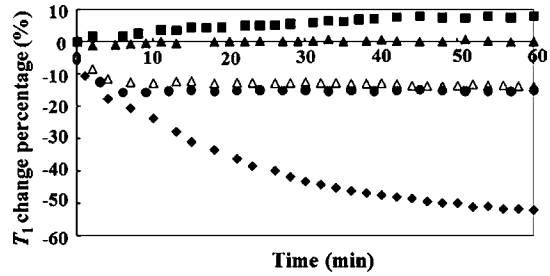

Figure 5. Change in T_1 (%) of [Gd(DOTA-FPβGu)] upon enzyme-catalyzed hydrolysis at 20 MHz, 37.0 ± 0.1 °C: (■) 0.5 mM [Gd(DOTA-FPβGu)] and 0.1 mg/mL β-glucuronidase in 100 mM PBS (pH = 7.4 ± 0.1); (▲) 0.5 mM [Gd(DOTA-FPβGu)] in 100 mM PBS; (●) 0.5 mM [Gd(DOTA-FPβGu)] and 0.5 mM HSA in 100 mM PBS; (△) 0.5 mM [Gd(DOTA-FPβGu)], 0.5 mM HSA and 0.01 mg/mL β-glucuronidase in 100 mM PBS; (♦) 0.5 mM [Gd(DOTA-FPβGu)], 0.5 mM HSA and 0.1 mg/mL β-glucuronidase in PBS.

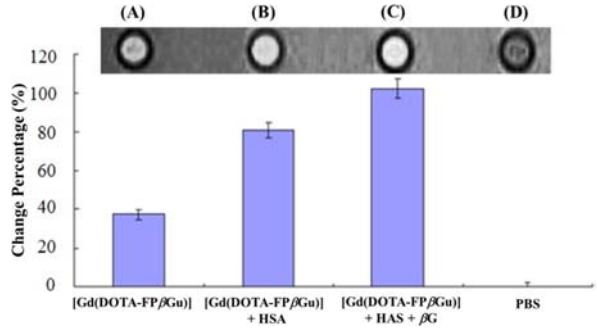

Figure 6. β-Glucuronidase-mediated enhancements of MR images: (A) 0.5 mM [Gd(DOTA-FPβGu)] in PBS; (B) 0.5 mM [Gd(DOTA-FPβGu)] and 0.5 mM HSA in PBS buffer; (C) 0.5 mM [Gd(DOTA-FPβGu)], 0.1 mg/mL β-glucuronidase, and 0.5 mM HSA in PBS buffer; (D) PBS alone.

expected, 15% decrease in longitudinal relaxation time was found in the presence of 0.5 mM HSA in PBS at pH = 7.4, indicating noncovalent interaction between native [Gd(DOTA-FPβGu)] and HSA. In addition, the T_1% does not change significantly in the presence of 0.5 mM HSA and 0.01 mg/mL of β-glucuronidase. This is due to low concentration of β-glucuronidase which hydrolyzes only a small fraction of [Gd(DOTA-FPβGu)]. Therefore, only few macromolecular adducts were formed in the above two cases. On the contrary, a 57% drop in T_1 value was observed at same HSA concentration as amounts of β-glucuronidase increased from 0.01 mg/mL to 0.1 mg/mL (Figure 5). Significantly more [Gd(DOTA-FPβGu)] was converted to [Gd(DOTA-FP)] and then conjugated to β-glucuronidase or HSA to form [Gd(DOTA-FP)]-HSA or [Gd(DOTA-FP)]-β-glucuronidase when higher concentration of β-glucuronidase was used. Therefore, the relaxation time (T_1) is significantly lower than those observed in the presence of HSA alone and in the presence of HSA and low concentration of β-glucuronidase. From the above results we conclude that [Gd(DOTA-FPβGu)] responds to β-glucuronidase

dx.doi.org/10.1021/ic301827p | Inorg. Chem. 2012, 51, 12426−12435

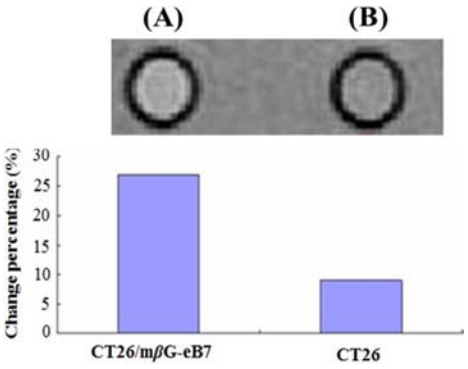

Figure 7. In *vitro* MR images of CT26/mβG-eB7 and CT26 cells and percent signal enhancement after incubating [Gd(DOTA-FPβGu)]: (A) CT26/mβG-eB7 cells incubated with [Gd(DOTA-FPβGu)](1 mM Gd); (B) CT26 cells incubated with [Gd(DOTA-FPβGu)] (1 mM Gd).

by changing relaxivity in a dose-dependent manner. Therefore, qualitative detection of β-glucuronidase can be performed by [Gd(DOTA-FPβGu)].

3.4. MR Imaging Studies of Enzymatic Activation of [Gd(DOTA-FPβGu)]. MR imaging was performed to evaluate the efficiency of [Gd(DOTA-FPβGu)] for detecting β-glucuronidase activity. The experiments were carried out on four cylindrical plastic containers. Figure 6 shows T_1-weighted MR images of [Gd(DOTA-FPβGu)] under three incubations: (A) [Gd-(DOTA-FPβGu)] alone, (B) [Gd(DOTA-FPβGu)] + HSA, (C) [Gd(DOTA-FPβGu)] + HSA + βG, and a control image from PBS alone, from left to right, respectively. The noncovalent interaction between [Gd(DOTA-FPβGu)] and HSA is reflected in the higher signal intensity of sample containing [Gd(DOTA-FPβGu)] and HSA than that of sample only containing [Gd(DOTA-FPβGu)]. The percentage change of signal intensity of [Gd(DOTA-FPβGu)] in the presence of β-glucuronidase and HSA is significantly higher than that of [Gd(DOTA-FPβGu)] in the PBS. These results are consistent with the relaxation time (T_1) experiments. In addition, *in vitro* MR image of cell lines overexpressing or moderately expressing β-glucuronidase further demonstrated the ability of [Gd(DOTA-FPβGu)] to detect the β-glucuronidase activity. As shown in Figure 7, higher MR signal intensity was observed at CT26/mβG-eB7 cells (express high levels of β-glucuronidase) than at CT26 cells (express moderate levels of β-glucuronidase).[28]

3.5. *In Vivo* MR imaging study. BALB/c mice bearing subcutaneous tumor xenografts of CT26 and CT26/mβG-eB7 tumors were tail-vein injected [Gd(DOTA-FPβGu)] or [Gd-(DTPA)]$^{2-}$ to test specific MR signal enhancement at tumors overexpressing β-glucuronidase. Stronger signal enhancement was noted in CT26/mβG-eB7 tumor regions when the mice were injected [Gd(DOTA-FPβGu)] (Figure 8). On the contrary, differential signal enhnacement between CT26 and CT26/mβG-eB7 tumors was lost when the tumor-bearing mice were injected [Gd-(DTPA)]$^{2-}$. Furthermore, after injection of [Gd(DOTA-FPβGu)]

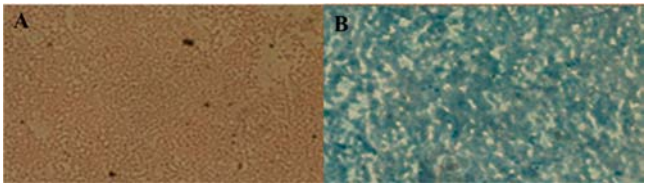

Figure 10. Enzyme histochemical analysis of (A) CT26 and (B) CT26/mβG-eB7 tumors stained with X-GlcA and nuclear fast red.

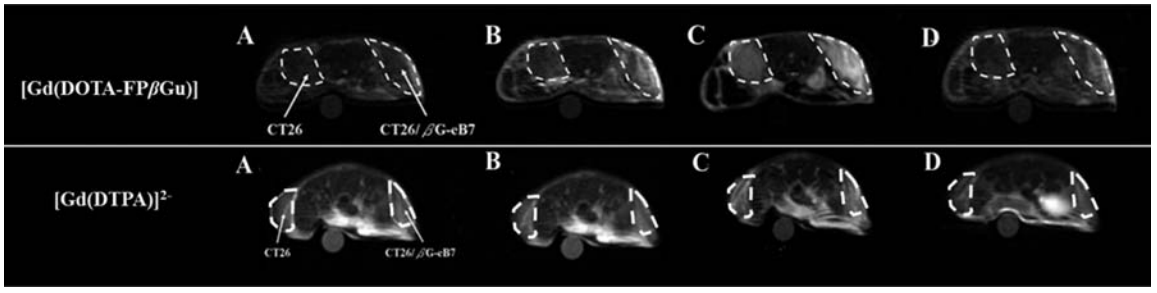

Figure 8. Representative T_1-weighted (TR/TE 100/13 ms) MR images of mice bearing CT26 and CT26/mβG-eB7 xenografts after injection of contrast agents. Upper panel shows mice injected with [Gd(DOTA-FPβGu)], and lower panel shows mice injected with [Gd(DTPA)]$^{2-}$: (A) precontrast images, or at (B) 5 min, (C) 10 min, (D) 90 min, after intravenous injection of 0.1 mmol/kg contrast agents.

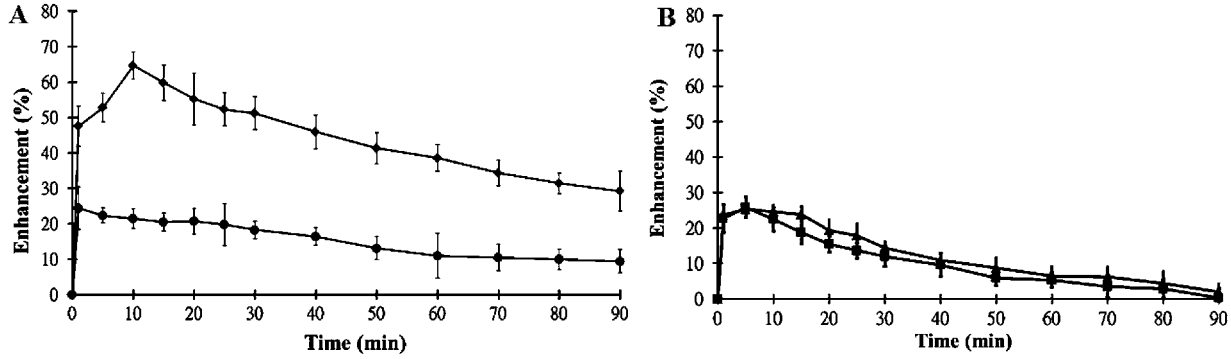

Figure 9. (A) Time course of signal enhancement (mean ± se) at CT26 (■) and CT26/mβG-eB7 (●) tumors after injection of [Gd(DOTA-FPβGu)]. Significantly higher enhancement can be noted in CT26/mβG-eB7 tumors. (B) Time-course of enhancement (mean ± se) of CT26 (■) and CT26/mβG-eB7 (●) tumors with [Gd(DTPA)]$^{2-}$. *P < 0.05 on posthoc comparison.

dx.doi.org/10.1021/ic301827p | *Inorg. Chem.* 2012, 51, 12426−12435

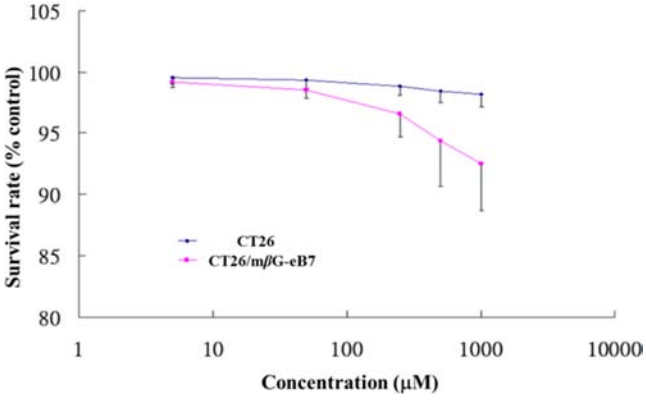

Figure 11. Cytotoxicity of [Gd(DOTA-FPβGu)] to CT26 and CT26/mβG-eB7. CT-26 and CT26/mβG-eB7 were incubated with graded concentrations of [Gd(DOTA-FPβGu)]. Cell viability was determined by the ATPlite luminescence ATP detection assay. Results represent the mean of results from 3 separate wells. Error bars show the standard error of the mean.

from tail vein the enhancement in MR signal intensity of CT26 and CT26/mβG-eB7 tumors rapidly rises, reaching a peak at one minute, and then declines steadily and slowly. Significant difference (ANOVA, $F = 187.5$, $P < 0.0001$) in enhancement of signal intensity can be found between tumor xenografts moderately and overexpressing β-glucuronidase at multiple time points after the injection of [Gd(DOTA-FPβGu)] (Figure 9). Differences in signal enhancement between tumors were lost throughout the entire study course when the mice were injected $[Gd(DTPA)]^{2-}$ (ANOVA, $F = 2.6$, $P = 0.11$). Finally, tumoral expression levels of β-glucuronidase were examined by X-GlcA staining of fresh tumor sections. In line with the imaging study, CT26/mβG-eB7 tumors expressed higher levels of β-glucuronidase than those of CT26 tumors *in vivo* (Figure 10).

3.6. Cytotoxicity of [Gd(DOTA-FPβGu)]. An imaging agent should display low toxicity before it could be used for *in vivo* studies. The survival of CT26 and CT26/mβG-eB7 cells after being treated with graded concentrations of [Gd(DOTA-FPβGu)] for 72 h were determined by the ATPlite luminescence. As shown in Figure 11, approximately 90% of CT26 cells survived even at 1000 μM of [Gd(DOTA-FPβGu)] which is relatively high concentration. The results demonstrated that the intact and active forms of [Gd(DOTA-FPβGu)] have low cell cytotoxicity.

4. CONCLUSION

A novel bioactivated pro-RIME MR imaging contrast agent, [Gd(DOTA-FPβGu)], was successfully synthesized. Extensive experimental studies demonstrate that [Gd(DOTA-FPβGu)] can be used for noninvasive visualization β-glucuronidase activity in the tumor tissues. Significant decrease in longitudional relaxation time was observed in the presence of β-glucuronidase and HSA. In addition, relaxometric studies reveal that T_1 relaxivity of [Gd(DOTA-FPβGu)] changes in response to the concentration of β-glucuronidase. The enzyme kinetic study shows that [Eu(DOTA-FPβGu)] is rapidly catalyzed and activated by β-glucuronidase. *In vitro* MR imaging signal intensity of β-glucuronidase-overexpressing cell line is 15% higher than that of a cell line expressing moderate levels of β-glucuronidase. Furthermore, *in vivo* evaluation of [Gd(DOTA-FPβGu)] for imaging β-glucuronidase in an animal tumor model was very encouraging. Therefore, we can conclude that [Gd(DOTA-FPβGu)] is a promising imaging agent for β-glucuronidase activity in tumors. This class of MR imaging contrast agents may greatly facilitate diagnosis and treatment of cancer in the future.

■ ASSOCIATED CONTENT

Supporting Information

HPLC chromatograms of DOTA-FPβGu and [Gd(DOTA-FPβGu)]. The E- and M-titration and Scatchard plot of [Gd(DOTA-FPβGu)]. This material is available free of charge via the Internet at http://pubs.acs.org.

■ AUTHOR INFORMATION

Corresponding Author

*E-mail: gcliu@kmu.edu.tw (G.-C.L.), ymwang@mail.nctu.edu.tw (Y.-M.W.). Phone: 886-7-3121101 ext 7701 (G.-C.L.), 886-3-5712121 ext 56972 (Y.-M.W.). Fax: 886-7-3154208 (G.-C.L.), 886-3-5729288 (Y.-M.W.).

Author Contributions

○These two authors contributed equally.

Notes

The authors declare no competing financial interest.

■ ACKNOWLEDGMENTS

The funding for the research was supported by National Science Council of Taiwan (Grants NSC 97-2314-B-037-038-MY3 and NSC 100-2113-M-009-002). This research was also particularly supported by "Aim for the Top University Plan" of the National Chiao Tung University and Ministry of Education, Taiwan, R.O.C. The authors thank Dr. Yi-Hsin Yang for her constructive advice on statistical analysis.

■ REFERENCES

(1) Lauffer, R. B.; Parmelee, D. J.; Dunham, S. U.; Ouellet, H. S.; Dolan, R. P.; Witte, S.; McMurry, T. J.; Walovitch, R. C. *Radiology* **1998**, *207*, 529.

(2) Caravan, P.; Cloutier, N. J.; Greenfield, M. T.; McDermid, S. A.; Dunham, S. U.; Bulte, J. W.; Amedio, J. C., Jr.; Looby, R. J.; Supkowski, R. M.; Horrocks, W. D, Jr.; McMurry, T. J.; Lauffer, R. B. *J. Am. Chem. Soc.* **2002**, *124*, 3152.

(3) Anelli, P. L.; Lattuada, L.; Lorusso, V.; Lux, G.; Morisetti, A.; Morosini, P.; Serleti, M.; Uggeri, F. *J. Med. Chem.* **2004**, *47*, 3629.

(4) Zhang, Z.; Greenfield, M. T.; Spiller, M.; McMurry, T. J.; Lauffer, R. B.; Caravan, P. *Angew. Chem., Int. Ed.* **2005**, *44*, 6766.

(5) Cheng, T. H.; Lee, W. T.; Jeng, J. S.; Wu, C. M.; Liu, G. C.; Chiang, M. Y.; Wang, Y. M. *Dalton Trans.* **2006**, *43*, 5149.

(6) Yang, J. J.; Yang, J.; Wei, L.; Zurkiya, O.; Yang, W.; Li, S.; Zou, J.; Zhou, Y.; Maniccia, A. L.; Mao, H.; Zhao, F.; Malchow, R.; Zhao, S.; Johnson, J.; Hu, X.; Krogstad, E.; Liu, Z. R. *J. Am. Chem. Soc.* **2008**, *130*, 9260.

(7) Moats, R. A.; Fraser, S. E.; Meade, T. J. *Angew. Chem., Int. Ed.* **1997**, *36*, 725.

(8) Louie, A. Y.; Hüber, M. M.; Ahrens, E. T.; Rothbächer, U.; Moats, R.; Jacobs, R. E.; Fraser, S. E.; Meade, T. J. *Nat. Biotechnol.* **2000**, *18*, 321.

(9) Hanaoka, K.; Kikuchi, K.; Terai, T.; Komatsu, T.; Nagano, T. *Chem.—Eur. J.* **2008**, *14*, 987.

(10) Nivorozhkin, A. L.; Kolodziej, A. F.; Caravan, P.; Greenfield, M. T.; Lauffer, R. B.; McMurry, T. J. *Angew. Chem., Int. Ed.* **2001**, *40*, 2903.

(11) Chang, Y. T.; Cheng, C. M.; Su, Y. Z.; Lee, W. T.; Hsu, J. S.; Liu, G. C.; Cheng, T. L.; Wang, Y. M. *Bioconjugate Chem.* **2007**, *18*, 1716.

(12) Chen, J. W.; Querol Sans, M.; Bogdanov, A., Jr.; Weissleder, R. *Radiology* **2006**, *240*, 473.

(13) Arena, F.; Singh, J. B.; Gianolio, E.; Stefanìa, R.; Aime, S. *Bioconjugate Chem.* **2011**, *22*, 2625.

(14) Abraham, R.; Barbolt, T. A. *Cancer Res.* **1978**, *38*, 2763.

(15) HariKrishna, D.; Rao, A. R.; Krishna, D. R. *Drug News Perspect.* **2003**, *16*, 309.
(16) Caldarella, A.; Buccoliero, A. M.; Marini, M.; Taddei, A.; Mennonna, P.; Taddei, G. L. *Pathol., Res. Pract.* **2002**, *198*, 109.
(17) Miller, B. F.; Kothari, H. V. *Exp. Mol. Pathol.* **1969**, *10*, 288.
(18) Curreri, P. W.; Kothari, H. V.; Bonner, M. J.; Miller, B. F. *Proc. Soc. Exp. Biol. Med.* **1969**, *130*, 1253.
(19) Floriańczyk, B.; Basińska, A.; Grzybowska-Szatkowska, L.; Mazurkiewicz, M.; Stryjecka-Zimmer, M. *Ann. UMCS* **2005**, *9*, 105.
(20) Florent, J. C., Monneret, C. *Anthracycline Chemistry and Biology II: Mode of Action, Clinical Aspects and New Drugs*; Springer-Verlag: Berlin, 2008; Vol. *283*, pp 99−140.
(21) Russell, R. I.; Watts, C. *Gut* **1968**, *5*, 585.
(22) Janda, K. D.; Lo, L. C.; Lo, C. H.; Sim, M. M.; Wang, R.; Wong, C. H.; Lerner, R. A. *Science* **1997**, *275*, 945.
(23) Gai, H. Z.; Kaden, T. A. *Helv. Chim. Acta* **1994**, *77*, 383.
(24) Kumar, K.; Chang, C. A.; Tweedle, M. F. *Inorg. Chem.* **1993**, *32*, 587.
(25) Kumar, K.; Sukumaran, K.; Chang, C. A.; Tweedle, M. F.; Eckelman, W. C. *J. Labelled Compd. Radiopharm.* **1993**, *33*, 473.
(26) McMurry, T. J.; Parmelee, D. J.; Sajiki, H.; Scott, D. M.; Ouellet, H. S.; Walovith, R. C.; Tyeklár, Z.; Dumas, S.; Bernard, P.; Nadler, S.; Midelfort, K.; Greenfield, M.; Troughton, J.; Lauffer, R. B. *J. Med. Chem.* **2002**, *45*, 3465.
(27) Chang, Y. H.; Chen, C. Y.; Singh, G.; Chen, H. Y.; Liu, G. C.; Goan, Y. G.; Aime, S.; Wang, Y. M. *Inorg. Chem.* **2011**, *50*, 1275.
(28) Su, Y. C.; Chuang, K. H.; Wang, Y. M.; Cheng, C. M.; Lin, S. R.; Wang, J. Y.; Hwang, J. J.; Chen, B. M.; Chen, K. C.; Roffler, S.; Cheng, T. L. *Gene Ther.* **2007**, *14*, 565.
(29) Lin, Y. H.; Dayananda, K.; Chen, C. Y.; Liu, G. C.; Luo, T. Y.; Hsu, H. S.; Wang, Y. M. *Bioorg. Med. Chem.* **2011**, *19*, 1085.
(30) Duimstra, J. A.; Femia, F. J.; Meade, T. J. *J. Am. Chem. Soc.* **2005**, *127*, 12847.
(31) *The Chemistry of Contrast Agents in Medical Magnetic Resonance Imaging*; To'th, E.; Helm, L.; Merbach, A. E., Eds.; John Wiley and Sons: New York, 2001; pp 45−119.
(32) Aime, S.; Anelli, P. L.; Botta, M.; Fedeli, F.; Grandi, M.; Paoli, P.; Uggeri, F. *Inorg. Chem.* **1992**, *31*, 2422.
(33) Zhang, X.; Chang, C. A.; Brittain, H. G.; Garrison, J. M.; Telser, J.; Tweedle, M. F. *Inorg. Chem.* **1992**, *31*, 5597.
(34) Weinmann, H. J.; Brasch, R. C.; Press, W. R.; Wesbey, G. E. *AJR, Am. J. Roentgenol.* **1984**, *142*, 619.